Unifying Approach to Modeling Granule Coalescence Mechanisms

A. A. Adetayo
E.I. DuPont de Nemours & Co., Wilmington, DE 19880

B. J. Ennis
E&G Associates, Nashville, TN 37215

A novel, physically based kernel for population balance modeling of granule growth by coalescence is presented. This kernel is size-independent in that all collisions with an effective average granule size less than a critical value are successful. Simulations based on this kernel show that a variety of contradictory experimental observations can be modeled. In the limiting case of viscoelastic collisions, the kernel can be related to the governing group of the Stokes number (Ennis et al., 1991), representing the ratio of granule collisional kinetic energy to viscous dissipation brought about by the binder. In more general cases, material properties that control deformability, such as interparticle friction, binder viscosity, and liquid content, strongly affect this critical size. The kernel clearly demonstrates the three regimes of drum granulation originally proposed by Kapur and Fuerstenau in 1964 and compares favorably with the two-stage sequential kernel developed by Adetayo et al. in 1995 for the drum granulation of fertilizers.

Introduction

Most process engineering problems involve mass and energy balances. However, in particulate processes, especially in cases where number rather than mass is of primary importance, a balance over the population of materials of a given size in the system is often necessary. The population balance is a statement of continuity that describes how the particle-size distribution changes with time and position (Hounslow et al., 1990). It is widely used to model formation and growth in a variety of processes such as crystallization (Randolph and Larson, 1988), granulation (Ennis, 1996; Ennis and Litster, 1997; Adetayo et al., 1995), pelletization (Sastry and Fuerstenau, 1970), and aerosol production (Landgrebe and Pratsinis, 1989). However, population balance modeling is not limited to particulate processes alone; it is also utilized in the areas of transport and chemical reaction engineering, as well as for dispersed-phase systems, and in particular for liquid–liquid dispersions. A review of the various applications of the population balance is given by Ramkrishna (1985).

For a batch, restricted-in-space, granulation system, the associated population-balance equation for modeling growth by coalescence alone is (Sastry and Fuerstenau, 1970):

$$\frac{\partial n(v,t)}{\partial t} = -\frac{1}{N(t)}\int_0^\infty \beta(v,u)n(u,t)n(v,t)\,du + \frac{1}{2N(t)}\int_0^v \beta(v-u,u)n(u,t)n(v-u,t)\,du, \quad (1)$$

where $n(v,t)$ is the number density function; u and v are the volumes of the coalescing granules; $N(t)$ is the total number of granules in the system at time t; and $\beta(v,u)$ is the coalescence kernel. The coalescence kernel is a very important parameter in the population balance equation. It is a measure of the frequency of successful coalescence following collision between two particles of volumes u and v. In general, the coalescence kernel can be subdivided into two parts (Sastry, 1975):

$$\beta(v,u) = \beta_o \beta^*(v,u). \quad (2)$$

The coalescence rate constant, β_o, affects the rate at which collisions result in successful coalescence and therefore, the average granule size. It is dependent on process operating

variables, such as bed agitation intensity and the degree of granule saturation, and material properties such as wettability and binder viscosity. $\beta^*(v,u)$ is an indication of the functional dependency of the kernel on the sizes of the coalescing granules. It determines the shape of the resultant granule-size distribution (Ennis and Adetayo, 1994; Adetayo, 1993; Smit et al., 1994).

Due to the complexity and limited knowledge of the forces involved in the granulation system, the form of the coalescence kernel for granulating materials is not yet established. In fact, one of the most difficult tasks in the application of the population balance is the determination of the form and nature of the coalescence kernel. This *inverse problem* is typically approached in two ways:

1. Finding the kernel or combination of kernels that provide the best fit to the experimental data (Ilievski, 1991; Adetayo et al., 1995; Hoornaert et al., 1994),
2. By the direct method (Tobin et al., 1990).

Elimination of candidate kernels is usually accomplished by comparing the characteristics of the kernel to the observed experimental trend of the size distribution. Typical characteristics commonly utilized are *gelling* or *nongelling* behavior (Smit et al., 1994), variance of the resultant granule-size distribution (broad or narrow) (Ennis and Adetayo, 1994; Adetayo et al., 1995; Hoornaert et al., 1994; Knight, 1994), and the self-preserving characteristics of the kernel (Kapur, 1972).

The wide variety of granule growth mechanisms and regimes that have been experimentally observed for coalescing particles makes modeling even more difficult. In the case of the drum granulation of limestone, for example, the classic work of Kapur and Fuerstenau (1964) demonstrated the existence of the three sequential growth regimes of nucleation, transition, and ball growth. Mechanisms of granule growth such as random coalescence, preferential coalescence, and crushing and layering have been proposed to explain the depicted growth behavior for each of these regimes. Ironically, no satisfactory explanation has been presented for why such regimes exist in the first place. In addition, these mechanisms and experimental observations are often contradictory and unique to only given classes of materials and processes. As an illustration, while Adetayo et al. (1993) observed that granule-size distribution initially narrows and then widens for the drum granulation of fertilizers, the reverse is observed for the drum granulation of limestone (Kapur and Fuerstenau, 1964). As with limestone, granule-size distribution usually widens and then narrows for the mixer granulation of pharmaceuticals (Kristensen et al., 1985). As a result of these observations, the current approaches to kernel development described earlier tend to recommend different kernels for different granulating systems and/or materials.

This article reviews the wide range of behavior that can be exhibited by previously proposed growth mechanisms and associated kernels for the batch granulation of particles undergoing growth by coalescence alone. This points out the misleading conclusions that can be drawn when attempting to infer the form of the growth kernel from the evolution of the size distribution. A different approach from previous modeling of the growth process is then taken by proposing a size-independent kernel such that only collisions with an effective size less than a characteristic value are successful. This approach combines the population-balance modeling works of Adetayo et al. (1995) and Ouchiyama and Tanaka (1975, 1982) with the microlevel work of Ennis et al. (1991), which considered the critical granule size capable of rebound from an elastic collision given the viscosity of the binding solution. This simple approach appears to unify the variety of previous observations regarding growth mechanisms.

Characteristics of Kernels of Varying Volumes

There is no analytical solution to the general form of Eq. 1. For the present study, the accuracy of the sectional-midpoint approximation proposed by Hounslow et al. (1990) is sufficient. This method discretizes the integrodifferential equation into a series of ordinary differential equations that are numerically solved with the fourth–fifth-order Runge-Kutta method (Fehlberg, 1970). The change in granule-size distribution is represented by

$$\frac{dN_i}{dt} = \frac{1}{N_t}\left(N_{i-1}\sum_{j=1}^{i-2} 2^{j-i+1}\beta_{i-1,j}N_j + \frac{1}{2}\beta_{i-1,i-1}N_{i-1}^2 - N_i\sum_{j=1}^{i-1} 2^{j-i}\beta_{i,j}N_j - N_i\sum_{j=i}^{\infty}\beta_{i,j}N_j \right), \quad (3)$$

where N_i is the number of particles in the ith interval. Note that a geometric discretization of the particle-size spectrum of $v_i = 2v_{i-1}$ is inherently built into Eq. 3.

The qualitative behavior of the growth process in terms of the resultant granule-size distribution is believed to be primarily controlled by the order of the kernel (Adetayo, 1993). For the specific case of coalescence, Kapur (1972) proposed a coalescence kernel $\beta(u,v)$ of the form:

$$\beta(u,v) = \beta_o\left[\frac{(u+v)^a}{(uv)^b}\right] \quad (4)$$

where u and v are the volumes of the coalescing granules, and β_o is the coalescence rate constant, which is a function of moisture content, granule material properties, and operating variables. The adjustable parameters a and b are chosen to model the observed growth patterns in a given process. For a and $b \neq 0$, the growth process is referred to as *preferential* coalescence, whereas for the case of $a = b = 0$, the kernel $\beta(u,v)$ becomes size-independent and growth is referred to as *random* coalescence. Equation 4 may be rewritten as

$$\beta(u,v) = u^{a-2b}f(v/u). \quad (5)$$

This gives an order δ, of $a-2b$. An example of the evolution of the size distribution for three cases of $a-2b <, =, > 0$ are depicted in Figures 1a–1c, where the normalized variance of the form of the coefficient of variation, $C.V.$, of the mass size distribution given by

$$C.V. = \sigma/d_{43} = \frac{\sqrt{\sum_i x_i(d_i - d_{43})^2}}{d_{43}} \quad (6)$$

is plotted against the mass mean diameter, d_{43}. Here, d_i and x_i are the average size and mass fraction of granules in the

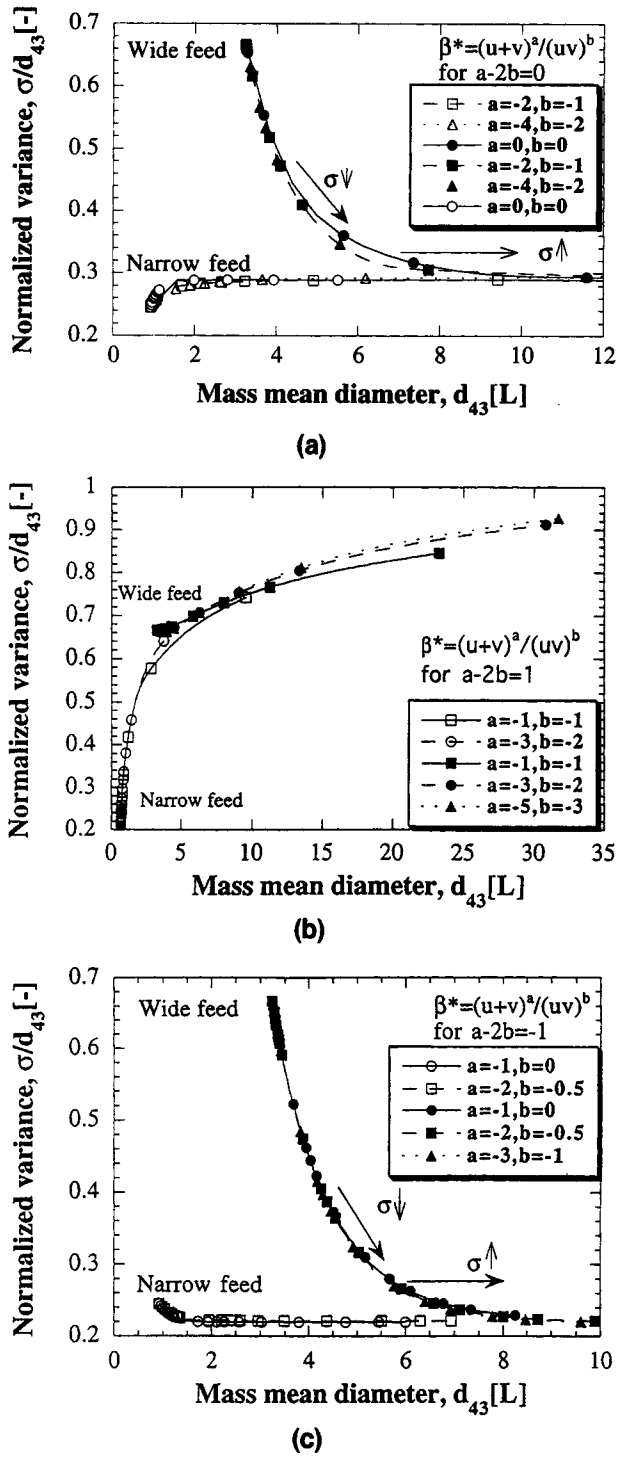

Figure 1. Evolution of the normalized variance with average size for (a) zero, (b) first, and (c) negative one order kernels.

ith size interval, respectively. The mass mean diameter is given by:

$$d_{43} = \frac{\sum_i N_i d_i^4}{\sum_i N_i d_i^3}.$$

Figure 1a illustrates the behavior of the zeroth-order kernels, $a - 2b = 0$. The instantaneous granule-size distribution for these kernels is observed to evolve along the same path as the specific case of random, size-independent growth ($a = b = 0$). (The rate of granule growth, of course, depends on the exact values of a and b.) As expected, the normalized variance for all kernels increases in time for a narrow feed distribution leveling out at the self-preserving value, at which point the *unnormalized* variance continues to increase in proportion to the mass mean diameter. When starting with a wide feed size distribution, however, the normalized variance decreases in time, again to the self-preserving value. The corresponding *unnormalized* variance, on the other hand, initially decreases but then increases as the size distribution approaches the self-preserving form at $d_{43} \sim 6 \pm 1$, which is not a unique size but depends on material properties and the initial size distribution. It should be noted that the initial drop in variance for wide initial distribution occurs over a time scale in which the average diameter approximately doubles. This drop was clearly observed in the work of Adetayo et al. (1993), which specifically focused on this region of growth. Other researchers, such as Kapur and Fuerstenau (1964) and Kristensen et al. (1985), apparently overlooked this region of growth, as they focused on changes of the order of multiples of the initial average diameter. Instead, they observed the expected increase in variance.

Figure 1b shows an example of the evolution of the variance for kernels of order 1. Equation 5 shows that all such kernels favor the growth of the largest granules, thereby leading to a widening of the size distribution, whether the initial feed size distribution is narrow or wide.

For kernels of order -1 as shown in Figure 1c, growth of the smallest granules is favored, promoting an initial narrowing of the size distribution for both wide and narrow feed distributions. The *C.V.* for the narrow feed distribution of Figure 1c is above that of the self-preserving distribution. Narrow feed distributions with a *C.V.* less than the self-preserving distribution would instead widen with time, approaching their self-preserving form as illustrated in Figure 1c.

From Figure 1, one can conclude that both the order of the kernel and the initial feed size distribution determine the shape and spread of the size distribution, at least for the examples with the general forms of kernels studied here. Both Figures 1b and 1c illustrate cases of growth by *preferential* Kernels. The initial narrowing of the granule size distribution illustrated by Figure 1c for kernels of order-1 corresponds to the later stage of growth of Kapur and Fuerstenau (1964) and of Kristensen et al. (1985). On the other hand, Figure 1b corresponds to the later stage of growth observed by Adetayo and coworkers for kernels of of order 1 where size distributions broaden with time. It would appear from the preceding that different kernels are needed to model each data set. In addition, it is not entirely clear why the later stages of the granulation of fertilizer should occur with a widening of the size distribution that cannot be modeled by a random kernel (Adetayo, 1993), whereas the granulation of the limestone can occur with either a narrowing or widening distribution, and the later stages of the mixer granulation of pharmaceutical powders narrow with time. In these cases, it appears necessary to introduce several kernels in order to model the entire

growth process (Adetayo et al., 1995; Hoornaert et al., 1994). In other words, although it is possible to model the growth behavior of a range of powders granulated by different processing techniques through judicious selection of the growth kernel, the question still remains as to why different growth patterns are observed. In addition, kernels with physical characteristics that are inconsistent with the nature of the process might provide the best fit. An example of this is the use of gelling kernels to model nongelling systems (Smit et al., 1994).

New Approach to Coalescence Kernel Development

Critical effective size

To reconcile the current situation, a new approach to kernel development is proposed. Rather than immediately resort to *probabilities* (Ouchiyama and Tanaka, 1982) or use an average characteristic of the distribution (Adetayo et al., 1995), one can approach the problem of coalescence from a deterministic point of view, and ask: What critical size of granule is capable of coalescence given its properties, the properties of the binding solution, and the collision velocity? Such an approach was initiated in the work of Ennis et al. (1991). By equating the viscous dissipation due to a binder layer to the initial kinetic energy of two colliding granules, Ennis and coworkers proposed that coalescence will occur if:

$$St \le St^*, \tag{7a}$$

where

$$St = (\rho D v)/16\mu \tag{7b}$$

and

$$St^* = \left(1+\frac{1}{e}\right)\ln(h/h_a). \tag{7c}$$

Here, St is a viscous Stokes number representing the initial kinetic energy of the granules made dimensionless with respect to the scale of viscous dissipation; ρ, μ, and v are the granule density, binder viscosity, and the initial collision velocity, respectively; D is the *harmonic mean* diameter of the two colliding granules; and St^* is the critical energy required for rebound (Barnocky and Davis, 1988). For the case of elastic collisions with a viscous coating that was originally considered, St^* is controlled by the ratio of binder layer thickness to asperity height (h/h_a) and the coefficient of restitution of the granules, e. It could in more general cases be determined by experiment, or calculated for collisions with different granule properties (Tardos, 1995). From Eq. 7, the critical combination of granule sizes capable of coalescence D^* is given by

$$D^* = \left(\frac{16\mu}{\rho v} St^*\right), \tag{8}$$

that is, for coalescence to occur,

$$D \le \left[\frac{16\mu}{\rho v} St^*\right]. \tag{9}$$

Equation 8 shows that D^* increases with ($\mu/\rho v$) as well as St^*. This was experimentally verified for noninertial processes (Adetayo et al., 1995). St^*, on the other hand, increases with liquid content. Thus D^* increases with the amount of *free liquid* available for coalescence. This is in agreement with experimental observation. Increasing the level of granule saturation increases both the rate and extent of granulation (Adetayo et al., 1993).

The Stokes analysis is used to determine the effect of operating variables and binder viscosity on *equilibrium* growth, where disruptive and growth forces are balanced. In the early stages of growth, in particular, for highly deformable systems, the Stokes analysis in its present form is inapplicable. Freshly formed, uncompacted granules are easily deformed, and as growth proceeds and consolidation of granules occur, they will surface harden and become more resistant to deformation. This increases the importance of the elasticity of the granule assembly. Therefore, in later stages of growth or for low deformability systems, granules approach the ideal Stokes model of rigid, elastic collisions. For these reasons, the Stokes approach has had reasonable success in providing an overall framework with which to compare a wide variety of granulating materials (Ennis, 1996; Ennis and Litster, 1997). In addition, the Stokes number controls in part the degree of deformation occurring during a collision, since it represents the importance of collision kinetic energy in relation to viscous dissipation, although the exact dependence of deformation on St is currently unknown.

Deformation physics

The ability of the granules to deform during processing increases the bonding or contact area, thereby dissipating breakup forces and has a large effect on growth rate. From a balance of binding and separating forces acting within the area of granule contact, Ouchiyama and Tanaka (1975, 1982) developed expressions for the probability of coalescence P given by:

$$\left(1-\frac{P^{1/n}}{\lambda}\right)^{3\zeta/2} = \left[(d_1 d_2)^{\gamma-3\eta/2}\Big/\left(\frac{d_1+d_2}{2}\right)^{2\gamma-4-3\eta/2}\right]\frac{1}{(D^*)^{4-3\eta/2}}, \tag{10}$$

where D^* is a characteristic limiting size above which coalescence becomes impossible.

$$D^* = (AQ^{3\zeta/2}K^{3/2}\sigma_T)^{1/(4-(3/2)\eta)} \tag{11}$$

and K is deformability, a proportionality constant relating the maximum compressive force Q to the deformed contact area. K is related to both the yield strength of the material, σ_y, that is, the ability of the material to resist stresses, and the ability of the surface to be strained without degradation or rupture of the granule (Kristensen et al., 1985). In general, high deformability K requires low yield strength σ_y and high critical strain $(\Delta L/L)_c$. Yield strength and critical strain in turn are a complex function of liquid loading, particle friction and size distribution, and binder viscosity, which has only recently been investigated (Iveson et al., 1994, 1996). σ_T is the tensile strength of the granule bond. The parameters ζ and η depend on the deformation mechanism acting within the con-

tact area, with their values bounded by the cases of complete plastic or complete elastic deformation. For plastic deformation, $\zeta = 1$, $\eta = 0$, and $K \propto 1/H$, where H is hardness. For elastic, Hertzian deformation, $\zeta = 2/3$, $\eta = 2/3$, and $K \propto (1/E^*)^{2/3}$, where E^* is reduced elastic modulus. In practice, granule deformation is often dominated by inelastic behavior of the contacts during collision, with surface deformability, replacing in part the role of viscosity in the approach of Ennis et al. (1991) as an energy dissipation mechanism. The parameters n, λ, and γ, as well as the bracketed term of Eq. 10, describe the number and types of forces acting on the contact region of the granules.

Cutoff kernel

For dynamic, plastic systems (i.e., $\zeta = 1$, $\eta = 0$), Eq. 10 becomes

$$\left(1 - \frac{P^{1/n}}{\lambda}\right)^{3/2} = \frac{D_{av}^4}{(D^*)^4}, \tag{12a}$$

where

$$D_{av} = (d_1 d_2)^{\gamma/4} \Bigg/ \left(\frac{d_1 + d_2}{2}\right)^{\gamma/2 - 1}. \tag{12b}$$

Here, D_{av} represents an effective average granule diameter for dynamic, plastic collisions, which is a generalization of the harmonic mean diameter D used in the Stokes analysis. Setting the probability of coalescence, $P = 0$, we obtain a generalized criterion of granule coalescence for dynamic, plastic systems:

$$D_{av} \le D^*. \tag{13}$$

Following the general form suggested by Eqs. 12 and 13, for coalescence to occur, we define an effective volume W as

$$W = \frac{(uv)^b}{(u+v)^a} \le W^*, \tag{14}$$

where a and b are model parameters that are expected to increase with the deformability of the granules, and W^* is the critical limit of granule volume capable of coalescence. To be dimensionally consistent,

$$2b - a = 1.$$

It should be noted that, for coalescence to occur,

$$W|_{u=v=u_c} = \frac{u_c}{2^a} \le W^* \tag{15a}$$

$$W|_{u \ll v} \Rightarrow \left[\frac{u}{v}\right]^b v \le W^* \tag{15b}$$

and

$$W|_{u<v} = \frac{\left[\frac{u}{v}\right]^b v}{\left[\frac{u}{v} + 1\right]^{2b-1}} \le W^*. \tag{15c}$$

Equations 15b and 15c show that coalescence of deformable granules will continue to occur as long as their size difference is big enough. This is in complete agreement with the observation of Ouchiyama and Tanaka (1975).

Evidently, a close relationship must exist between this critical granule volume W^* and the observed kernels in Eq. 4. Bearing this in mind, one could consider all granule collisions where the *effective* mean volume $W = (uv)^b/(u+v)^a$ is less than the critical volume W^* as successful. Therefore, growth could be modeled by a size-independent kernel, β_0. All effective volumes W greater than W^* are considered unsuccessful, having a zero rate of growth. This critical volume, W^*, also referred to as the *cutoff size* in other parts of this article, is expected to vary with both the binder and material properties, and can be determined by an approach similar to that that led to the Stokes number criterion. In addition, the Stokes number criterion as it currently stands is seen to give a first-order approximation of the cutoff size for the case of rigid, elastic collisions. The population balance equation (Eq. 1) then becomes

$$\frac{\partial n(v,t)}{\partial t} = -\frac{1}{N(t)} \int_0^\infty U(W^* - W)|_{u,v} n(u,t) n(v,t)\, du + \frac{1}{2N(t)} \int_0^v U(W^* - W)|_{v-u,u} n(u,t) n(v-u,t)\, du, \tag{16}$$

where $U(W^* - W)$ is the unit-step function given by

$$U(W^* - W) = \begin{cases} \beta_o & W \le W^* \\ 0 & W > W^*. \end{cases} \tag{17}$$

The next subsection shows that it is possible to model a myriad of observed granulation behavior with this simple approach. In addition, while a and b are still empirical constants, they bear a closer physical relationship to the process of granule collision, deformation, and subsequent coalescence. That is, in principle, they are measurable quantities.

Characteristics of the cutoff kernel

Figures 2a and 2b depict the evolution of the average granule diameter and normalized variance with time for both narrow and wide feed size distributions. Here, a and b are taken to be 3 and 2, respectively. These values are equivalent to using a typical value of $\gamma = 8$ (Ouchiyama and Tanaka, 1982) in Eq. 12b. A range of behavior is observed. The evolution of the granule-size distribution is a complex function of the width of the feed size distribution and the position of this distribution with respect to self-preserving growth and the critical effective volume W^*. From Eq. 14a, the values of W^* of 0.01 and 0.4 chosen here correspond to average diameters of approximately 0.5 and 2, respectively. Size distributions that lie well *below* W^* evolve in a manner similar to that governed by a constant kernel. For example, as illustrated for a narrow feed and $W^* = 0.4$, the variance increases with average diameter d_{43} and then levels off at $d_{43} \sim 2$ (see Figure 1a). Similarly, the feed with a wide size distribution and $W^* = 0.4$ decreases until $d_{43} \sim 5$. (Again, see Figure 1a for comparison.) Note here that the wide feed has a substantial portion of its size distribution below the critical average volume of $W^* = 0.4$.

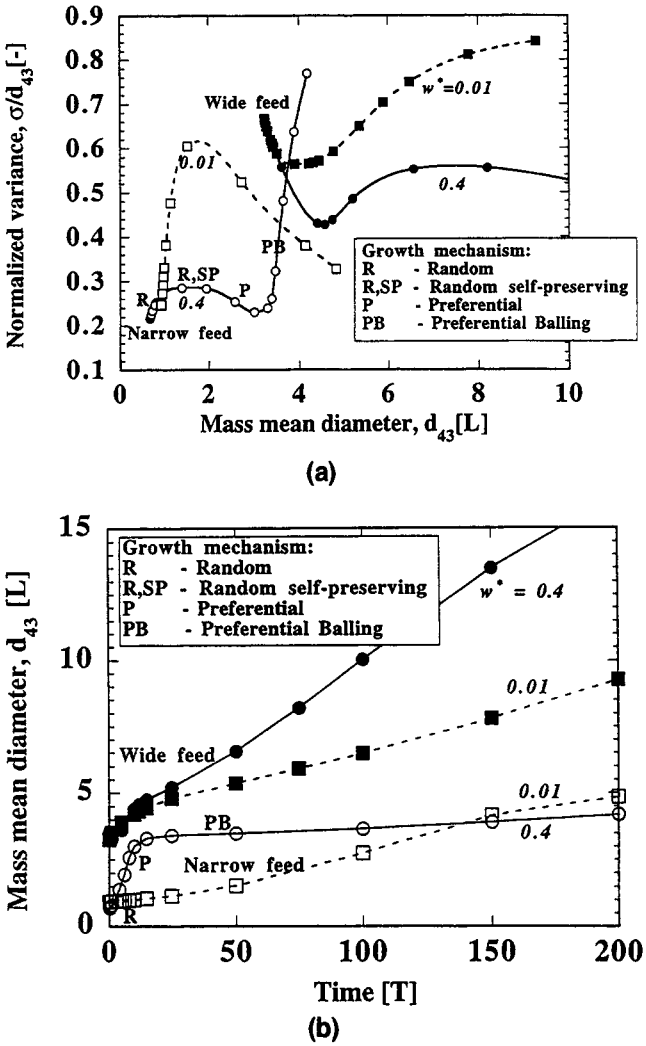

Figure 2. (a) Evolution of variance with average size using Eq. 16 and $w=(uv)^2/(u+v)^3$; (b) evolution of average size with time using Eq. 16 and $w=(uv)^2/(u+v)^3$.

As the narrow feed for $W^* = 0.4$ continues to grow with $d_{43} > 2$, the variance drops since much of the distribution now lies above the critical effective size. This behavior for narrow feeds clearly corresponds to experimental observations in which preferential coalescence leads to a narrowing of the distribution following a random growth regime. As the size distribution continues to evolve for $W^* = 0.4$, the variance goes through a minimum and then rapidly increases while the average diameter d_{43} continues to increase, but at a much slower rate. The bend in the diameter growth curve of Figure 2b for $W^* = 0.4$ and narrow feed corresponds to the minimum in the variance curve of Figure 2a. This trend is similar in characteristic to the balling region of Kapur and Fuerstenau (1964), or the coating region of Ennis et al. (1991). In this preferential ball growth region, only the larger granules are capable of coalescing with the small ones, since the middle of the distribution has exceeded the critical volume. Inevitably, a point is reached where only the largest of granules, which are very few in number, can grow. The variance must again fall and terminate at a particular point. This fall in variance is illustrated for the second case of narrow feed where the critical size is lowered to $W^* = 0.01$. In fact, the narrow feed with $W^* = 0.01$ lies entirely within the balling region, since nearly all the distribution lies well above the critical effective size W^*. This is also evident from its slow rate of growth in Figure 2b. The various growth regimes are indicated for the case of narrow feed and $W^* = 0.4$.

Wide distributions typically narrow with time initially due to random growth with sizes in excess of self-preserving, but also display a later widening of the distribution for the values of W^* studied here, due to the preferential ball growth regime. Again, the minimum in the variance curves of Figure 2a correspond to the bends in the diameter growth curves of Figure 2b. This trend is observed in the drum granulation work of Adetayo et al. (1993).

Experimental Examples

Limestone granulation

Examples of the evolution of the median granule size with time for various cutoff kernels are presented in Figure 3a. Shown in comparison are curves for the constant kernels of equivalent rate constants, β_o. As expected, deviations from predictions of the constant kernels begin to occur near the cutoff points, that is, at a D_{50} coinciding with the size at which particles of equal size rebounds. For example, for $W^* = 10$, Eq. 15 predicts that particles of diameters 3.36 for $a = 1$, and 6.1 for $a = 3.6$, cannot coalesce with another particle of equal size. The insert in Figure 3a shows the experimental data from Kapur (1972). Excellent qualitative agreement exists between the cutoff kernel and these earlier data upon which their granulation regimes of nucleation, transition, and balling were based.

Regimes of granulation

Figure 3b shows another interesting phenomenon. Here the number based mean size (d_{10}) is plotted against time for an arbitrary "narrow" initial size distribution. Shown in comparison are the experimental data of Kapur and Fuerstenau (1964). Due to the nonavailability of their initial-size distribution, detailed modeling is not possible. However, an attempt was made to choose an initial-size distribution with a d_{10} similar to that of Kapur and Fuerstenau (1964). For the purpose of qualitative comparison, their time scale was rescaled by a factor of 1.86 to account for differences in rate constants. This notwithstanding, Figure 3b shows good agreement between the predictions from Eq. 16 and the experimental data. The transitions between the granulation regimes of random, preferential, and preferential ball growth as presented by Kapur and Fuerstenau (1964) are clearly evident in Figure 3b.

In summary, Figures 3a and 3b demonstrate the unique ability of the cutoff kernel (Eq. 16) to simulate all the stages of granule growth by coalescence. No single kernel previously available has demonstrated this ability. Also, the cutoff kernel has the ability to simulate multistaged kernels (Figure 3b).

Fertilizer granulation

Having established the fact that this new approach to kernel development can be used to model a range of seemingly contradictory experimental observations, we now further

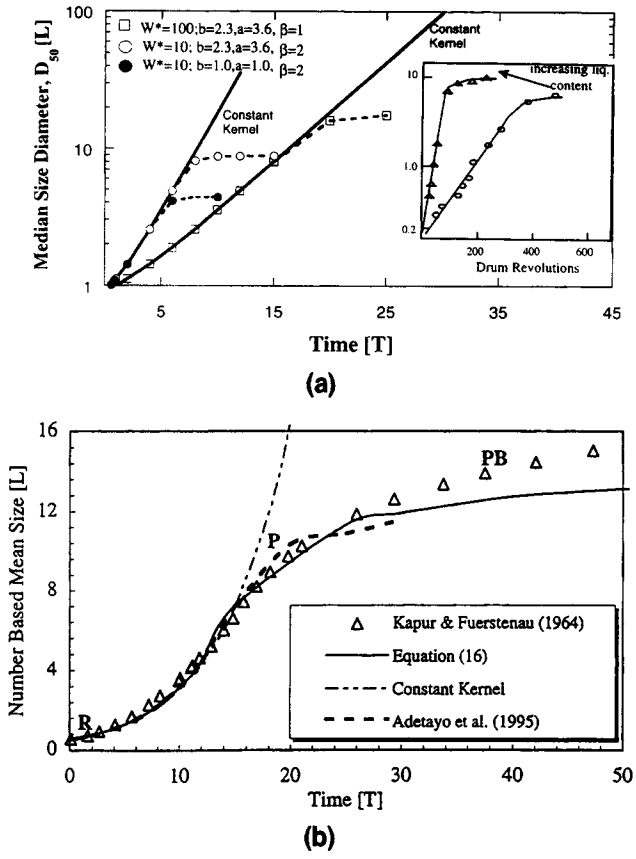

Figure 3. (a) Effect of varying the cutoff size and its parameters on the median granule size (Inset: Data of Kapur, 1972); (b) three stages of granulation, Eq. 16 compared to the data of Kapur and Fuerstenau (1964).

demonstrate its utility by examining three sets of data from the fertilizer granulation work of Adetayo et al. (1995). The cumulative size distributions for the granulation of diammonium phosphate (DAP) at 5, 15, and 25 min are depicted in Figures 4 to 6 for two moisture levels and two initial distributions. It was previously shown (Adetayo, 1993) that no available kernel in the literature can, by itself, completely model

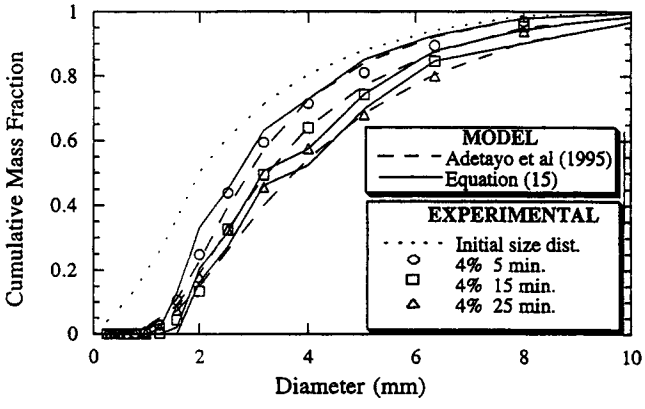

Figure 4. Comparison of model predictions with experimental data of DAP at 4% moisture (Adetayo et al., 1993).

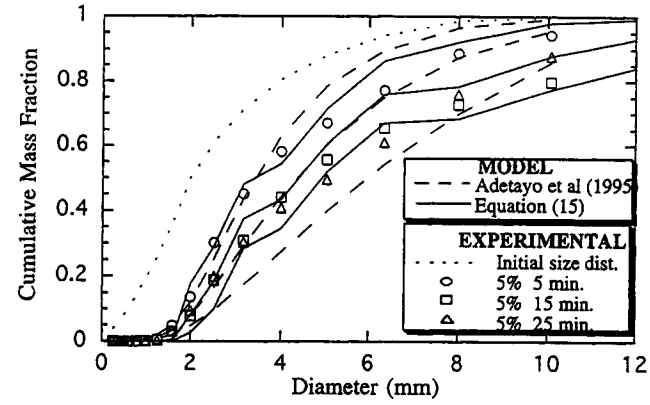

Figure 5. Comparison of model predictions with experimental data of DAP at 5% moisture (Adetayo et al., 1993).

these results. A two-stage sequential kernel was needed to adequately model these data. Figures 4 and 5 demonstrate the performance of both Eq. 16 ($W^* = 0.08$, $a = 3.0$), and the sequential, two-stage kernel (Adetayo et al., 1995) in modeling the experimental granulation data. Within experimental error, both models are in excellent agreement with the DAP data. Figure 5 illustrates that the cutoff kernel of Eq. 16 gives a slightly better fit to the granule-size distribution with 5% moisture content at long granulation times, for example, 25 min. In addition, Figure 6 shows that the cutoff kernel gives an excellent fit to the experimental data for a much broader initial-size distribution (Adetayo et al., 1993). Care must be taken when comparing the results from the sequential kernel and Eq. 16. While the sequential kernel was used in a predictive sense, Eq. 16, being in a preliminary stage, is only used to fit these experimental data.

Conclusions

A complex relationship exists between initial feed distribution, granule properties, and the mechanism of granulation. This has led to the inevitable development of a variety of granule growth mechanisms and regimes which are often unique to a given class of material and process. This in turn has necessitated the development of several models for different systems.

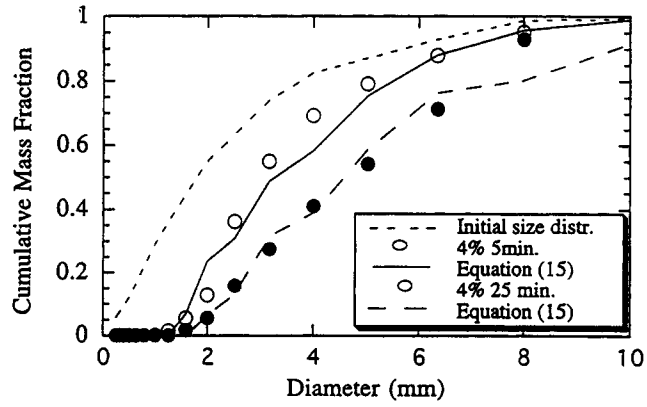

Figure 6. Fit of Eq. 16 to a much broader initial size distribution (type III DAP initial size distribution of Adetayo et al., 1993).

To address this state of coalescence modeling, a novel approach to kernel development has been proposed. The approach is deterministic in nature with respect to the effect of granule size on growth, and assumes all collisions with a combination of granule volume less than some critical cutoff size are successful. Growth can then be modeled by a constant kernel with a cutoff size, W^*. Simulation studies based on this approach show that a range of previously observed granulation behavior can be successfully modeled, giving the potential to unify the different experimental observations in the literature. In addition, the approach has a physical basis and can be linked to the earlier microlevel studies of Ennis et al. (1991) as well as later studies that related the random kernel to process operating variables and the formulation of material properties (Adetayo et al., 1995), thereby making first-principle granulation process design feasible.

The proposed cutoff kernel compares favorably with the two-stage, sequential kernel developed by Adetayo et al. (1995) for the drum granulation of fertilizers, and at least qualitatively agrees with the limestone granulation data of Kapur (1972). A simulation using the cutoff kernel clearly demonstrates the three stages of granulation (Kapur and Fuerstenau, 1964; Ennis et al., 1991), a characteristic that has hitherto never been demonstrated by a single kernel.

Simulations show that W^* has a strong and complex effect on the characteristics of the granule-size distribution for a given feed size distribution, since it is strongly affected by the granule's deformability, which is not yet fully understood. Because we have only a qualitative understanding of how W^* varies with process and material variables, a quantitative relationship is still needed before the model can be used in a predictive way. Work is currently underway to establish this.

Acknowledgments

The authors acknowledge with appreciation the fruitful, illuminating discussions regarding the Stokes number regimes and analysis with J. D. Litster of the University of Queensland and G. Tardos of The City College of New York.

Notation

A = deformed contact area, L^2
D_{50} = median diameter, L
d_{10} = number-based average size, L
h = binder layer thickness
h_a = granule's surface asperity
k = frequency of collision factor
v_i = upper volume of the ith interval, L^3

Literature Cited

Adetayo, A. A., "Modeling and Simulation of a Fertilizer Granulation Circuit," PhD Thesis, Dept. of Chemical Engineering Univ. of Quennsland, Brisbane, Australia (1993).

Adetayo, A. A., J. D. Litster, and M. Desai, "Effect of Process Variables on Granulation of Fertilizers with Broad Initial Size Distribution," *Chem. Eng. Sci.*, **48**, 3951 (1993).

Adetayo, A. A., J. D. Litster, S. E. Pratsinis, and B. J. Ennis, "Population Balance Modeling of Drum Granulation of Materials with Wide Size Distributions," *Powder Tech.*, **82**, 37 (1995).

Barnocky, G., and R. H. Davis, "Elastohydrodynamic Collision and Rebound of Spheres: Experimental Verification," *Phys. of Fluids*, **31**, 1324 (1988).

Ennis, B. J., "Agglomeration and Size Enlargement: Session Summary Paper," *Powder Tech.*, **88**, 203 (1996).

Ennis, B. J., and A. A. Adetayo, "On the Unification of Granule Coalescence Mechanisms: A New Approach," *Int. Part. Tech. Forum*, Denver, CO, p. 271 (1994).

Ennis, B. J., and J. D. Litster, "Section 20: Size Enlargement," *Perry's Chemical Engineers Handbook*, 7th ed., McGraw-Hill, New York (1997).

Ennis, B. J., G. I. Tardos, and R. Pfeffer, "A Microlevel Based Characterization of Granular Phenomena," *Powder Tech.*, **65**, 257 (1997).

Fehlberg, E., "Low Order Classical Runge-Kutta Formulas with Step-Wise Control," *Computing*, **6**, 61 (1970).

Hoornaert, F., G. Meesters, S. Pratsinis, and B. Scartlett, "Powder Agglomeration in a Lodige Granulator," *Int. Part. Tech. Forum*, Denver, CO, p. 278 (1994).

Hounslow, M. J., R. L. Ryall, and V. R. Marshall, "A Discretized Population Balance for Nucleation, Growth and Aggregation," *AIChE J.*, **34**, 1821 (1990).

Ilievski, D., "Modelling $Al(OH)_3$ Agglomeration during Batch and Continuous Precipitation in Supersaturated Caustic Aluminate Solutions," PhD Thesis, Univ. of Queensland, Qld., Australia (1991).

Iveson, S., J. D. Litster, and B. J. Ennis, "Fundamental Studies of Granule Consolidation," *Proc. Australian Chem. Eng. Conf., I. Chem. E.*, CHEMECA (1994); *Powder Tech.*, **88**, 15 (1996).

Kapur, P. C., "Kinetics of Granulation by Non-Random Coalescence Mechanism," *Chem. Eng. Sci.*, **27**, 1863 (1972).

Kapur, P. C., and D. W. Fuerstenau, "Kinetics of Green Pelletisation," *Trans. AIME*, **229**, 348 (1964).

Knight, P. C., "A Study of Agglomeration Using a High Shear Mixer," *Int. Part. Tech. Forum*, Denver, CO, p. 231 (1994).

Kristensen, H. G., P. Holm, and T. Schaefer, "Mechanical Properties of Moist Agglomerates in Relation to Granulation Mechanisms, I & II," *Powder Tech.*, **44**, 227 (1985).

Landgrebe, J. D., and S. E. Pratsinis, "Gas-Phase Manufacture of Particulates: Interplay of Chemical Reaction and Aerosol Coagulation in Free Molecular Regime," *Ind. Eng. Chem. Res.*, **28**, 1474 (1989).

Ouchiyama, N., and T. Tanaka, "Probability of Coalescence in Granulation Kinetics," *Ind. Eng. Chem. Proc. Des. Dev.*, **14**(3), 286 (1975).

Ouchiyama, N., and T. Tanaka, "Kinetic Analysis and Simulation of Batch Granulation," *Ind. Eng. Chem. Proc. Des. Dev.*, **21**, 29 (1982).

Ramkrishna, D., "The Status of Population Balances," *Rev. Chem. Eng.*, **3**, 49 (1985).

Randolph, A. D., and M. A. Larson, *Theory of Particulate Processes*, 2nd ed., Academic Press, New York (1988).

Sastry, K. V. S., "Similarity Size Distribution of Agglomerates during their Growth by Coalescence in Granulation or Green Pelletization," *Int. J. Min. Process.*, **2**, 187 (1975).

Sastry, K. V. S., and D. W. Fuerstenau, "Size Distribution of Agglomerates in Coalescing Disperse Phase Systems," *Ind. Eng. Chem. Fundam.*, **9**, 145 (1970).

Smit, D. J., M. J. Hounslow, and W. R. Paterson, "Aggregation and Gelation: I. Analytical Solutions for CST and Batch Operation," *Chem. Eng. Sci.*, **7**, 1025 (1994).

Tardos, G., *Proc. Annu. Fine Particles Society Meeting*, Fine Particles Society, Chicago (1995).

Tobin, T., R. Muralidar, H. Wright, and D. Ramkrishna, "Determination of Coalescence Frequencies in Liquid Dispersions: Effect of Drop Size Dependence," *Chem. Eng. Sci.*, **45**, 3491 (1990).

Manuscript received Jan. 10, 1996, and revision received Dec. 2, 1996.